

RESEARCH PAPER

Rubisco *in planta* k_{cat} is regulated in balance with photosynthetic electron transport

H. Eichelmann, E. Talts, V. Oja, E. Padu and A. Laisk*

Department of Plant Physiology and Biophysics, Institute of Molecular and Cell Biology, University of Tartu, Riia 23, Tartu 51010, Estonia

Received 19 May 2009; Revised 8 July 2009; Accepted 13 July 2009

Abstract

Site turnover rate (k_{cat}) of Rubisco was measured in intact leaves of different plants. Potato (*Solanum tuberosum* L.) and birch (*Betula pendula* Roth.) leaves were taken from field-growing plants. Sunflower (*Helianthus annuus* L.), wild type (wt), Rubisco-deficient (–RBC), FNR-deficient (–FNR), and Cyt b_6/f deficient (–CBF) transgenic tobacco (*Nicotiana tabacum* L.) were grown in a growth chamber. Rubisco protein was measured with quantitative SDS-PAGE and FNR protein content with quantitative immunoblotting. The Cyt b_6/f level was measured *in planta* by maximum electron transport rate and the photosystem I (PSI) content was assessed by titration with far-red light. The CO_2 response of Rubisco was measured *in planta* with a fast-response gas exchange system at maximum ribulose 1,5-bisphosphate concentration. Reaction site k_{cat} was calculated from V_m and Rubisco content. Biological variation of k_{cat} was significant, ranging from 1.5 to 4 s^{-1} in wt, but was $>6 \text{ s}^{-1}$ at 23 °C in –RBC leaves. The lowest k_{cat} of 0.5 s^{-1} was measured in –FNR and –CBF plants containing sufficient Rubisco but having slow electron transport rates. Plotting k_{cat} against PSI per Rubisco site resulted in a hyperbolic relationship where wt plants are on the initial slope. A model is suggested in which Rubisco Activase is converted into an active ATP-form on thylakoid membranes with the help of a factor related to electron transport. The activation of Rubisco is accompanied by the conversion of the ATP-form into an inactive ADP-form. The ATP and ADP forms of Activase shuttle between thylakoid membranes and stromally-located Rubisco. In normal wt plants the electron transport-related activation of Activase is rate-limiting, maintaining 50–70% Rubisco sites in the inactive state.

Key words: Photosystem I, Rubisco, Rubisco activase.

Introduction

Rubisco (ribulose 1,5-bisphosphate carboxylase/oxygenase, EC 4.1.1.39) is a dominant rate-controlling enzyme of photosynthetic CO_2 assimilation, along with diffusion resistances in leaves. Rubisco is a regulated enzyme, its activity level being the result of a complicated balance between activation/deactivation.

An assembled Rubisco holoenzyme, consisting of eight small (14 kDa) and eight large (53 kDa) (Knight *et al.*, 1990) subunits containing eight active sites, requires carbamylation of a Lys residue by a non-substrate CO_2 followed by binding of Mg^{2+} for activation (Badger and Lorimer, 1976; Boyle and Keys, 1987). Binding of the substrate RuBP to the

uncarbamylated enzyme blocks the activation process (Jordan *et al.*, 1983). Protonation during the enediolization of RuBP bound to the carbamylated enzyme may generate different 5C phosphates that block the active site (Edmondson *et al.*, 1990a, b). Several phosphorylated compounds bind to Rubisco sites and act as dead-end inhibitors (Parry *et al.*, 2008). In many plants 2-carboxyarabinitol-1-phosphate (CA1P) is synthesized from 2-carboxyarabinitol which binds to the active site with high affinity precluding enzyme activation (Vu *et al.*, 1984; von Caemmerer and Quick, 2000).

Rubisco activase (henceforth referred to as Activase) catalyses the carbamylation and releases inhibitory sugar

* To whom correspondence should be addressed: E-mail: alaisk@ut.ee

Abbreviations: CA1P, carboxyarabinitol-1-phosphate; C_c , CO_2 concentration at the Rubisco active sites; FRL, far-red light (720 nm); PFD, PAD, photon flux density ($\mu\text{mol quanta m}^{-2} \text{ s}^{-1}$), incident and absorbed, respectively; PSII and PSI, photosystems II and I; P700, donor pigment of PSI; Activase, Rubisco activase; Rubisco, ribulose-1,5-bisphosphate carboxylase/oxygenase; RuBP, ribulose 1,5-bisphosphate; wt, wild type.

© 2009 The Author(s).

This is an Open Access article distributed under the terms of the Creative Commons Attribution Non-Commercial License (<http://creativecommons.org/licenses/by-nc/2.5/uk/>) which permits unrestricted non-commercial use, distribution, and reproduction in any medium, provided the original work is properly cited.

phosphates from uncarbamylation or carbamylated sites (Salvucci *et al.*, 1987; Portis Jr, 1992; Portis, 2003). Activase is bound to Rubisco as an oligomer of up to 14 subunits, exhibiting ATPase activity (Robinson and Portis, 1989; Lilley and Portis, 1997). Activase is inhibited by ADP, hence the ATP/ADP ratio is a sensitive regulator of Rubisco activation state. In most plants there are two isoforms of Activase. Distinct from the smaller isoform (41–44 kDa), the larger isoform (45–46 kDa) is regulated by the ferredoxin-thioredoxin f system (Zhang and Portis, 1999; Zhang *et al.*, 2002).

For some time it has been understood that, in plants growing under saturating light and optimal temperature, Rubisco is nearly fully activated. This notion emerged from the fact that the activation state (ratio) measured *in vitro* accurately matched the carbamylation ratio (Butz and Sharkey, 1989), and usually 80–90% of Rubisco sites are carbamylated under these optimal conditions (Cen and Sage, 2005; Yamori *et al.*, 2006). At moderately high temperatures (30–40 °C) Activase is progressively unable to cope with the increasing rate of Rubisco inactivation, so the carbamylation (=activation) state decreases (Quick *et al.*, 1991a; Cen and Sage, 2005; Sharkey, 2005; Yamori *et al.*, 2006). These observations supported the notion that carbamylation by Activase is the major regulator of Rubisco activity—until variable activity of the presumably fully carbamylated enzyme was observed.

When extracted Rubisco protein was precipitated with sulphate ions and redissolved and carbamylated in a phosphate-free medium, the resulting ‘maximal activity’ was greater than the ‘total activity’ of the carbamylated enzyme before the precipitation. Precipitation evidently released an unknown inhibitor from carbamylated or uncarbamylated sites (Parry *et al.*, 1997). When the Activase content was gradually decreased in anti-sense transgenic tobacco, the number (or *in planta* turnover rate) of carbamylated sites decreased finally about 10-fold (He *et al.*, 1997; Parry *et al.*, 2003). Similar impairment of the function of Rubisco was observed under the influence of moderately high temperatures in these anti-sense plants (Sharkey *et al.*, 2001). Early experiments on lysed chloroplasts (Campbell and Ogren, 1990, 1992), as well as Cyt *b6/f*-deficient and GAPDH-deficient tobacco (Ruuska *et al.*, 2000), revealed that activation of the Activase is not a simple function of the ATP/ADP ratio, but is somehow related to Cyt *b6/f* content and PSI electron transport, demonstrating the importance of further *in planta* investigations.

A convenient metric of enzyme activity is k_{cat} , the catalytic turnover rate of an active site. Extracted Rubisco from C_4 plants exhibited the highest k_{cat} of 4.86 ± 0.89 at 28 °C, followed by 3.55 ± 0.54 of Rubisco from C_3 plants from cool habitats and 2.46 ± 0.52 s^{-1} of Rubisco from C_3 plants from warm habitats (Sage, 2002). Such variation of k_{cat} values could indicate an evolutionary adjustment (Tcherkez *et al.*, 2006), but the active sites could be differently inhibited as well. The balance of Rubisco inhibitors and activators is best revealed directly *in planta*. An experimental difficulty is that Rubisco V_m can not be measured in normal wild-type leaves,

because photosynthesis becomes limited by RuBP regeneration far below the V_m of Rubisco. This problem was elegantly bypassed by using Rubisco-deficient transgenic plants, where Rubisco was rate-limiting over a wide range of CO_2 concentrations (von Caemmerer *et al.*, 1994). In these leaves k_{cat} was 3.53 s^{-1} at 25 °C, but was estimated to be 4.24 s^{-1} after the carbamylation ratio of 0.8 at 1500 μmol quanta m^{-2} s^{-1} was taken into account. The latter k_{cat} value is higher than most reported values in C_3 plants.

The CO_2 response curve of Rubisco was measured *in planta* at CO_2 concentrations up to at least three times $K_m(CO_2)$ by accumulating RuBP at low CO_2 and O_2 concentrations and then measuring the initial rate of CO_2 fixation after a rapid increase in CO_2 concentration (Laisk and Oja, 1998; Laisk *et al.*, 2002). The biological variation of k_{cat} was wide. It decreased from 4 to 2.5 s^{-1} with increasing Rubisco content in sunflower grown under different conditions (Eichelmann and Laisk, 1990). In mature birch (*Betula pendula*) leaves the average k_{cat} was about 2 s^{-1} (Eichelmann *et al.*, 2004a). In developing birch leaves Rubisco V_m increased in proportion to the capacity of the developing photosynthetic machinery, k_{cat} varied from 1.35 to 2.24 s^{-1} (Eichelmann *et al.*, 2004b). In *Betula pendula* and *Tilia cordata* leaves growing in a natural canopy the apparent k_{cat} values were 2.3 and 1.6 s^{-1} , respectively, independent of sun/shade exposure in the vertical cross-section of the canopy (Laisk *et al.*, 2005), all cited measurements at 22.5 °C). Significant correlation was detected between the amount of activated Rubisco (V_m) and PSI density, suggesting that the activity of Activase is related to the photosynthetic electron transport system.

This overview shows that in normally photosynthesizing leaves Rubisco is present in high quantities, but the variable k_{cat} values reflect partial enzyme activation. It is likely that the stromal redox state and ATP/ADP ratio are not the only parameters controlling Rubisco activation via Activase; an, as yet, unknown inhibitor controls the number of Rubisco sites that can be activated by carbamylation. In this work, the actual Rubisco activity *in planta*, as a function of the amount of holoenzyme and in relation to the photosynthetic light reactions, is investigated. It is shown that the activation state of Rubisco is generally low in wild-type plants containing high Rubisco levels. It is still low in N-starved leaves where Rubisco content is low, but PSI content is low as well. It is even lower in FNR-deficient and Cyt *b6/f*-deficient tobacco leaves containing normal amounts of Rubisco, but impaired in electron transport capacity. Rubisco activation state approaches the maximum in transgenic leaves containing little Rubisco but sufficient PSI. In these leaves, the catalytic turnover rate of an active Rubisco site may exceed 6 s^{-1} at 22.5 °C.

Materials and methods

Plant material

Birch (*Betula pendula* Roth.) leaves were taken either from young trees growing in open top chambers in Suonenjoki,

Finland (the control trees for CO₂ and ozone enrichment experiments, Eichelmann *et al.*, 2004a, b) or from full-grown trees in a natural community in Järvelja, Estonia (Laisk *et al.*, 2005). The petioles of excised leaves were immersed in water and leaves were fitted to the measuring chamber. Potato (*Solanum tuberosum* L.) was grown in pots in the field and in the laboratory (Laisk *et al.*, 2007). Wild-type (wt), Rubisco-deficient (–RBC, Hudson *et al.*, 1992) and Cyt *b₆f* deficient (–CBF, Price *et al.*, 1995) transgenic lines of tobacco (*Nicotiana tabacum* L.) cv. W38 were kindly supplied by Professor D Price (Australian National University, Canberra). The FNR-deficient (–FNR) tobacco line (Hajirezaei *et al.*, 2002) was kindly supplied by Professor U Sonnewald (Gatersleben, Germany). The transgenic and corresponding reference wt tobacco plants were grown in 4l pots and nutrient-rich soil. In the N gradient (–N series) wt tobacco plants were grown hydroponically at Ca(NO₃)₂ concentrations of 100, 50, 25, 20, 17, 12, and 5% of the standard Knop level. In all cases the laboratory growth conditions were PFD of 300–400 μmol quanta m^{–2} s^{–1} and a 12/12 h 25/20 °C day/night cycle. Three full-grown attached leaves (positions 5–7) were used in measurements for the –N series. The transgenic leaves were measured over a wider age range, resulting in highly variable Rubisco contents.

Gas exchange measurement system

The gas exchange measurement system (Laisk and Oja, 1998; Laisk *et al.*, 2002) was designed to vary incident quantum flux densities and chamber CO₂ and O₂ concentrations and to measure fast transitions in transpiration, CO₂ uptake and O₂ evolution rates, Chl fluorescence, and 810 nm transmittance (oxidized plastocyanin and P700⁺). The leaf chamber of 32 mm diameter and 3 mm height was illuminated through a multi-arm light guide by two Schott KL 1500 tungsten halogen lamps (Schott GmbH, Mainz, Germany), providing actinic white light and saturation pulses of 11 000 μmol m^{–2} s^{–1}. CO₂ exchange was measured with an infrared CO₂ analyser LI-6251 (Li-Cor, Inc. Lincoln, NE, USA) and transpiration was measured with a micropsychrometer incorporated in the gas stream. Intercellular air space and chloroplast CO₂ concentrations are represented as equivalent liquid phase molarities.

Incident quantum flux density was measured with a quantum sensor (LI-250, Li-Cor, Inc. Lincoln, NE). Leaf absorbance of white and far-red light (FRL) was measured using an integrating sphere and a spectroradiometer PC-2000 (Ocean Optics, Dunedin, FL).

Measurement of Rubisco protein

A disc of 1.86 cm² was excised from the leaf part that had been enclosed in the gas-exchange chamber. The disc was ground in liquid nitrogen and homogenized in 0.8 ml of 50 mM MES–NaOH buffer (pH 6.8) containing 20 mM MgCl₂, 50 mM 2-mercaptoethanol, and 1% (w/w) Tween-80 (all from Sigma-Aldrich, St Louis, MO, USA). Part of

the homogenate was diluted with the SDS-PAGE loading buffer and incubated in a boiling water bath for 5 min. Such samples were kept at –20 °C until SDS-PAGE. The gels were stained with Coomassie Serva Blue G and scanned with UMAX Power Look III scanner in the light transmission mode and resolution of 500 dpi. The Rubisco large subunit band was denoted by a freehand line and the optical density of the selected area was integrated in the red colour channel using updated ImageQuant™ software considering the logarithmic relationship between the scanner signal and optical density. The SDS-PAGE sample volume was increased for extracts anticipated to contain less Rubisco, with the aim of adjusting the optical density of the band within the range of the calibration bands (three calibration bands were run in each gel along with samples). Performing the extraction procedure on the precipitate did not liberate any Rubisco.

The gels were calibrated using a known mass of Rubisco purified from young sunflower leaves grown with excess nutrients. Leaves (100 g) were ground in liquid nitrogen and extracted with 240 ml of extraction buffer. The homogenate was filtered, centrifuged, and proteins were sedimented from the supernatant at first with 37% and then with 50% (NH₄)₂SO₄. The sediment was dissolved and desalted with a Sephadex G-25 column. The fraction containing protein (48 ml) was subjected to chromatography with a DEAE-Toyopearl column and a 0.025–0.6 M NaCl gradient. Fractions containing Rubisco were collected and the protein was sedimented with 65% ammonium sulphate. The pellet was dissolved in 25 ml of buffer and desalted with Sephadex G-25. Equal volumes of the Rubisco fraction and buffer were dried at 90 °C in two repetitions. The mass of Rubisco was obtained by difference. Aliquots of the Rubisco preparation were stored in liquid N₂ and used later as standards during SDS-PAGE. The standard was about 95% pure Rubisco.

The Rubisco active site turnover rate k_{cat} was calculated as

$$k_{\text{cat}} = \frac{550\,000 V_{\text{m}}}{8 m_{\text{RBC}}}, \quad (1)$$

where 550 000 is the molecular weight assumed to be invariant among plant species (www.brenda.uni-koeln.de) and m_{RBC} is the Rubisco concentration (g m^{–2}). Possible small differences in the molecular weight of Rubisco from different species were neglected in these experiments.

Measurement of photosystem I density

PSI density was measured by oxidative titration of the PSI donor side using a known rate of absorption of FRL (Oja *et al.*, 2003). In order to avoid interference by reduced plastocyanin and cyclic electron transport (both donating additional electrons to P700, thus slowing down the rate of its oxidation), measurements were carried out near the steady-state FRL level. The speed of P700 re-oxidation under FRL after a brief dark exposure is an exponential

process. The product of the PAD of FRL ($\mu\text{mol absorbed quanta m}^{-2} \text{ s}^{-1}$) and exponential time constant $\tau(\text{s})$ yields the PSI density N_1 ($\mu\text{mol m}^{-2}$):

$$N_1 = \tau \text{PAD}_{\text{FRL}}. \quad (2)$$

Equation (2) is based on a self-evident assumption that a larger pool of P700 requires a longer time for oxidation by a given FRL photon fluence rate, assuming the quantum efficiency is constant [close to 100% (Hiyama, 1985)]. The PSI densities were checked by reductive titration using O_2 evolution measurement (Oja *et al.*, 2004). The leaf was illuminated under FRL, a single-turnover flash of white light was applied and FRL was immediately turned off. The number of electrons generated by PSII was measured as four times the integral of O_2 evolution after the flash. Electrons arriving at the PSI donor side via Cyt *b₆f* caused partial reduction of the PSI donors P700^+ and PC^+ . The extent of this fast reduction was relatively greater when the number of PSI donor side carriers was smaller and vice versa; hence, the number of PSI m^{-2} was deduced from this relationship (Oja *et al.*, 2004). The S-states of the water-splitting complex were randomized due to the slow PSII excitation caused by FRL.

The *in planta* PSI density measurements were carried out with a PAM-101 fluorometer equipped with an emitter/detector unit ED P700DW (H. Walz GmbH, Effeltrich, Germany), redesigned for the wavelength difference of 810–950 nm. Far-red light (720 nm) was provided by a light-emitting diode source (Fast-Est Instruments, Tartu, Estonia) equipped with a longpass filter to minimize PSII excitation. Single turnover flashes were produced by a xenon arc flash lamp MVS 7060 (Perkin Elmer, Salem, MA, USA). O_2 evolution produced by an individual flash was measured at very low ambient O_2 concentration of 10–50 $\mu\text{mol mol}^{-1}$ with a zirconium cell analyser S-3A (Ametek, Pittsburgh, PA, USA). The incident PFD of FRL was measured with the spectroradiometer PC-2000 calibrated in absolute units against a standard lamp.

The *in planta* measurements of PSI density were also compared to *in vitro* redox titrations of PSI density in thylakoid preparations, based on the known differential optical extinction coefficient between oxidized and reduced P700 at 700 nm [$64 \text{ mM}^{-1} \text{ cm}^{-1}$ (Hiyama and Ke, 1972)]. Leaf discs (1.86 cm^2) were ground and washed in buffer (1 ml per 1 leaf disc) containing 50 mM MES-KOH (pH 7.0), 10 mM NaCl, 5 mM MgCl_2 , and 300 mM sorbitol. Triton-X100 was added after washing to a final concentration of 1% (all reagents from Sigma-Aldrich, St Louis, MO, USA). Finally, 20 mg polyvinyl pyrrolidone (PVPP) per leaf disc was added to avoid interference from phenolic compounds. Starch particles, PVPP and suspended plant material were sedimented by centrifugation at 3000 *g* for 5 min. Part of the thylakoid suspension (supernatant) was oxidized with 40 mM ferricyanide and the rest of the solution was reduced with 40 mM Na-ascorbate. The difference spectrum of these solutions was measured in a UV-2410PC spectrophotometer (Shimadzu Corporation, Kyoto Japan). The entire procedure, except optical meas-

urements, was carried out on ice. Parallel determinations based on all three methods were proportional (data not shown), but the *in vitro* method tended to show somewhat more PSI than the two rather well-coinciding *in planta* optical titrations.

Quantitative immunoblotting of ferredoxin-NADP reductase

Leaf discs (3.72 cm^2) were ground in 300 μl of buffer containing 50 mM TRIS-HCl (pH 7.0), 5 mM MgCl_2 , 5 mM dithiothreitol, 2 mM EDTA, and 0.5 mM phenylmethanesulphonyl fluoride (PMSF). Protein extract of each sample corresponding to 5 mg leaf fresh weight was mixed with SDS-PAGE sample buffer and heated by boiling in a water bath for 3 min. Proteins were concentrated in a 5% stacking gel and separated by 12% SDS-PAGE. Immunoblotting was performed using standard protocols (Burnette, 1981). Pre-stained protein markers were run in neighbouring lanes. FNR was detected immunologically by sheep anti-FNR (dilution 1:10 000), and visualized using the appropriate IgG secondary antibody conjugated with horseradish peroxidase (dilution 1:20 000, Sigma) and the chemiluminescence method (GE Healthcare, UK). Band intensities were quantified (Quantity One, Bio-Rad). Three separate blots were made of each sample and the band intensities were averaged and normalized to the most intense sample. On average, the ratio of FNR protein in the –FNR plants to wt was 0.41, with the lowest of 0.23 and highest of 0.77 of wt.

Measurement of leaf N content

The content of organic N in leaves was measured with the micro-Kjeldahl method (Kjeltech Auto 1030, Foss Tecator AB, Hoeganaes, Sweden).

Results

Rubisco kinetic curves in planta

Gas exchange and optical measurement routines were essentially the same as used before (Laisk *et al.*, 2002). Maximal RuBP pool levels accumulated in leaves at an ambient CO_2 concentration of 200 $\mu\text{mol mol}^{-1}$ and O_2 concentration of 20 mmol mol^{-1} . Fast transitions were made from this steady-state to lower and higher CO_2 concentrations. At lower CO_2 concentrations the RuBP pool did not change and the initial slope of the CO_2 response of Rubisco kinetics was measured in the steady-state. During the jumps to higher CO_2 concentrations RuBP regeneration became rate-limiting and the RuBP pool began to decrease after the transition. The fast-response gas exchange measurement system correctly recorded the CO_2 uptake rate beginning from 2 s after the transition. The CO_2 uptake associated with CO_2 solubilization and bicarbonate formation was recorded in a parallel measurement carried out in the dark. The time-course of the carboxylation rate was obtained by subtracting the trace recorded in the dark

from the trace recorded in the light. The initial carboxylation rate was obtained by extrapolating the carboxylation rate to the moment of the CO_2 increase. The initial carboxylation rate was plotted against the chloroplast CO_2 concentration C_c calculated considering this initial rate and the diffusion resistances in the gas phase, r_{gw} , and in the liquid phase of mesophyll cells, r_{md} . The latter was determined using the electron transport method of Harley *et al.* (1992), considering the reduction of alternative acceptors. These Rubisco kinetic curves were rectangular hyperbolae with $K_m(\text{CO}_2)$ of $10 \mu\text{M}$ at a leaf temperature of 22.5°C (Fig. 1), in close accordance with earlier *in vitro* (Yokota and Kitaoka, 1985) and *in planta* (von Caemmerer *et al.*, 1994; Laisk *et al.*, 2002) measurements. In wt plants the maximum reaction rate, V_m , of Rubisco (approaching $100 \mu\text{mol CO}_2 \text{ m}^{-2} \text{ s}^{-1}$, calculated by extrapolating the rectangular hyperbola to an infinitely high CO_2 concentration) was considerably faster than the maximum steady-state CO_2 - and light-saturated rate of photosynthesis, A_m . In the Rubisco-deficient transgenic plants V_m was about equal to A_m , indicating that, in these plants, photosynthesis was Rubisco-limited at all CO_2 concentrations. In $-\text{FNR}$ and $-\text{CBF}$ plants, as in wt plants, the V_m of Rubisco, though low, was still higher than the steady-state photosynthetic rate.

Leaf N and Rubisco content

The growth of wt tobacco plants at different nutrient solution N contents and the selection of leaves of different age from control wt plants and from $-\text{RBC}$, $-\text{FNR}$, and $-\text{CBF}$ plants resulted in different N contents in leaves. Rubisco content was generally higher at higher leaf N,

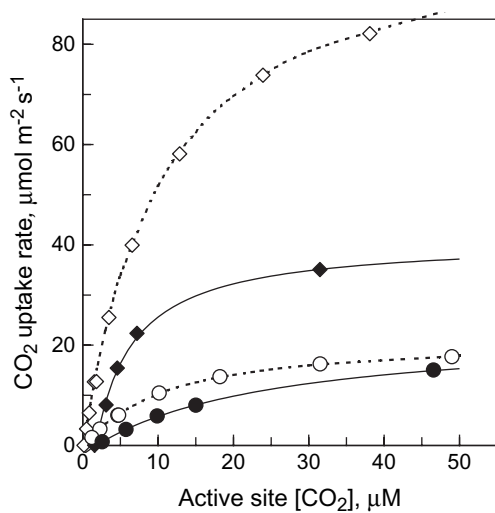


Fig. 1. Steady-state CO_2 response curves of CO_2 uptake at $210 \text{ mmol O}_2 \text{ mol}^{-1}$ (filled data points, solid line) and kinetic curves of Rubisco with respect to active site CO_2 concentration at $20 \text{ mmol O}_2 \text{ mol}^{-1}$ (empty data points, dotted line) in wild-type (diamonds) and $-\text{RBC}$ (circles) tobacco. Jumps of CO_2 concentration down and up were made from the steady-state (duplicate empty diamond 4th from zero).

however, the slope of the regression was different in different treatments (Fig. 2). The least variable dependence was obtained in the $-\text{N}$ series, where Rubisco content increased linearly with N content, with a small offset on the N axis. At any leaf N content the Rubisco level of the $-\text{RBC}$ plants was far below that of wt plants, but neither $-\text{FNR}$ nor $-\text{CBF}$ plants exhibited Rubisco deficiency.

Rubisco content and k_{cat}

Among the leaves examined, Rubisco content ranged from very low values to a maximum of $80 \mu\text{mol active sites m}^{-2}$. The interdependence between k_{cat} and Rubisco content was reciprocal (Fig. 3). In the mutants with extremely low Rubisco content (and young sunflower leaves transferred from low to high growth light) k_{cat} exceeded 6 s^{-1} . In wt tobacco plants the highest k_{cat} values were 4 s^{-1} detected in leaves with low Rubisco content. At high Rubisco levels k_{cat} values were about 2 s^{-1} over the range of active site concentrations of $50\text{--}70 \mu\text{mol m}^{-2}$ in wt tobacco, potato, and birch leaves. The following empirical regression equation models the reciprocal dependence between Rubisco site content and the apparent (average) k_{cat} assuming the maximum k_{cat} of 4.3 s^{-1} as recorded for wt plants.

$$k_{\text{cat}} = \frac{4.3}{1 + 0.03 \text{RBC}}, \quad (3)$$

where RBC is the active site concentration ($\mu\text{mol m}^{-2}$).

Notably, the $-\text{FNR}$ and $-\text{CBF}$ tobacco leaves exhibited about the same Rubisco content as wt leaves, but their k_{cat} values were only 0.5 s^{-1} , significantly lower than in wt plants with similar Rubisco content. A closer analysis of Fig. 4A shows a significant correlation ($R^2=0.9$) between Rubisco k_{cat} and the relative expression level of FNR in different plants. The transgenic down-regulation of $\text{Cyt } b_6$

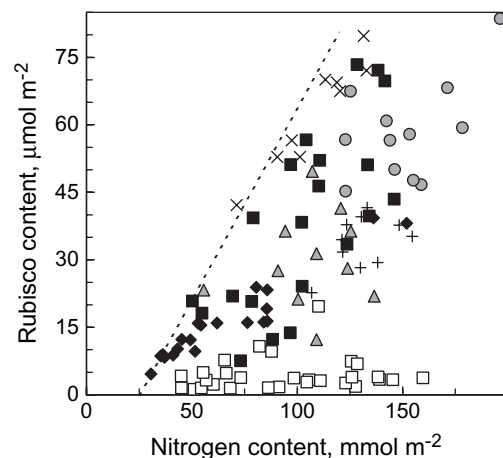


Fig. 2. The dependence of Rubisco content on leaf N content. Filled black and grey data points, wild type; empty data points, transgenic plants. Filled triangles, sunflower; filled circles, potato; filled squares, wt tobacco; filled diamonds, wt $-\text{N}$ tobacco; open squares, $-\text{RBC}$ tobacco; multi, $-\text{FNR}$ tobacco; plus, $-\text{CBF}$ tobacco. Dashed line indicates the maximum slope of regression.

was characterized by the exponential rate constant (reciprocal of the time constant) of post-illumination re-reduction of P700⁺. As with -FNR plants, a similarly high correlation was observed between Rubisco k_{cat} and PSI electron transport rate in the -CBF tobacco (Fig. 4B).

PSI density and k_{cat}

Assuming that PSI density proportionally characterizes the capacity of other components of the electron transport chain (Graan and Ort, 1984) and that Activase is functionally related to ATP synthase, one may expect that more Rubisco is activated in leaves exhibiting a higher ratio of PSI per Rubisco active site. The content of PSI increased with leaf N (Fig. 5). A plot of Rubisco k_{cat} versus the ratio of PSI per Rubisco active site site exhibited a saturating

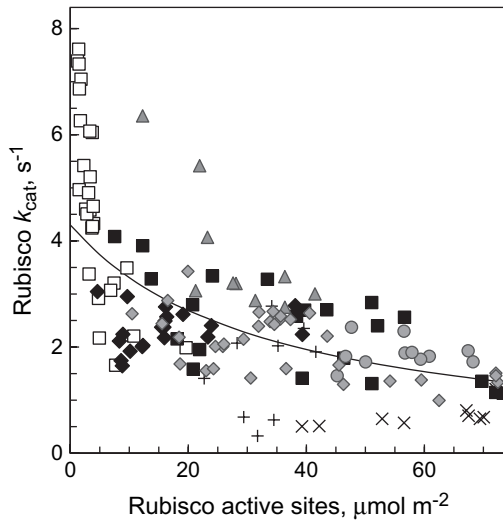


Fig. 3. Average *in planta* catalytic turnover rate, k_{cat} , of Rubisco sites as a function of the Rubisco content in leaves. Grey diamonds, data for birch from Laisk *et al.* (2005) and Eichelmann *et al.* (2004b); the meaning of the other symbols is given in Fig. 2. Sunflower leaves (grey triangles) with exceptionally high k_{cat} were transferred from low to high growth light. The line was calculated from equation (3).

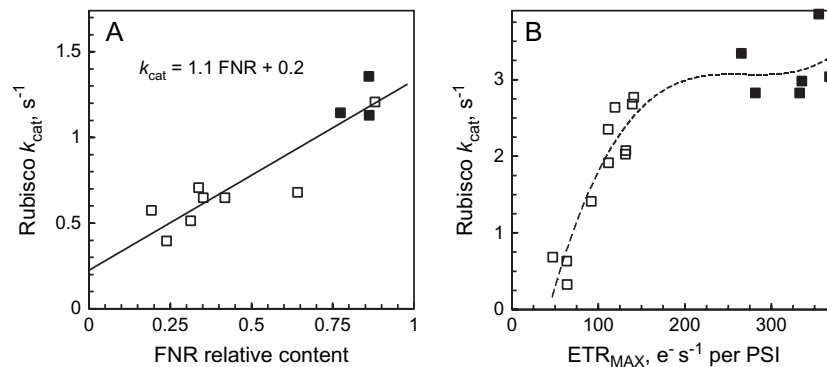


Fig. 4. Average *in planta* catalytic turnover rate, k_{cat} , of Rubisco sites as a function of relative FNR content in the -FNR (A) and of maximum electron transport rate ETR_{MAX} in -CBF (B) transgenic tobacco (empty symbols). Filled symbols present comparative wt plants from the same growth series.

relationship, where data points for wt plants formed the initial slope (low PSI/Rubisco) and data from the -RBC plants formed the saturation phase (high PSI/Rubisco, Fig. 6A). The hyperbolic relationship of equation (4) describes the dataset involving the maximal k_{cat} of 8 s⁻¹ recorded for -RBC plants:

$$k_{\text{cat}} = \frac{8 \left(\frac{\text{PSI}}{\text{RBC}} \right)}{0.085 + \left(\frac{\text{PSI}}{\text{RBC}} \right)}. \quad (4)$$

The initial part of the relationship is represented better in the reciprocal plot of Fig. 6B. In the latter, data from the -FNR and -CBF plants fall below the average of the wt plants, indicating that, in these plants, Rubisco is significantly less activated than expected, based on the average PSI/Rubisco ratio (in some -CBF plants Cyt *b₆f* level was only slightly down-regulated and, thus, did not influence Rubisco k_{cat}). Equation (5) approximates the reciprocal relationship:

$$k_{\text{cat}} = \frac{8}{1 + 0.085 \left(\frac{\text{RBC}}{\text{PSI}} \right)}. \quad (5)$$

Discussion

Measurement of the *in planta* k_{cat} of Rubisco

The reported k_{cat} values are based on the V_m of Rubisco, measured *in planta*, divided by the content of Rubisco active sites in leaves. Therefore, the k_{cat} values represent an average over all the Rubisco active and inactive sites, and therefore do not characterize a distinct biochemical species. The *in planta* method of measurement of the initial rate of CO₂ fixation by RuBP-saturated Rubisco was first used by Laisk and Oja (1974) and later by Ruuska *et al.* (1998). Reliable CO₂ fixation rates by RuBP-saturated Rubisco could be measured at CO₂ concentrations of at least 3 $K_m(\text{CO}_2)$ (up to 75% of V_m) in wt plants (at higher CO₂ concentrations the pre-accumulated RuBP was carboxylated too fast), but full kinetic curves could be measured

with high precision in $-RBC$ plants, where the Rubisco content was low. Thus, reliability of the reported k_{cat} values is mainly dependent on the measurement of Rubisco protein.

The amount of Rubisco was measured by quantitative SDS-PAGE calibrated gravimetrically, which is the most straightforward method to detect Rubisco protein. For example, the widely used method of binding radioactive carboxyarabinitol bisphosphate (CABP) requires a correction factor of unknown origin and constancy, considering that about 6.5 CABP molecules are bound per Rubisco instead of 8 (Butz and Sharkey, 1989; Sage and Seemann, 1993). A potential problem with the gel measurements used here was the occurrence of unidentified bands that comigrate with the Rubisco large subunit. This could cause an overestimation at the lowest Rubisco levels. However, overestimation of Rubisco would lead to an underestimation of the highest k_{cat} values. Underestimation of Rubisco levels (resulting in overestimated k_{cat}) could occur if some Rubisco was so tightly bound to the membrane system that

it did not extract despite the stringent procedure employed (Makino and Osmond, 1991).

In our leaves Rubisco density varied from 2 to 70 $\mu\text{mol sites m}^{-2}$, similar to the range reported for wt and $-RBC$ tobacco measured by the CABP-binding method (von Caemmerer *et al.*, 1994; Kubien and Sage, 2008). The maximum Rubisco density is also not substantially different from the value of 64 $\mu\text{mol sites m}^{-2}$ measured in rice using a similar quantitative electrophoresis method (Makino *et al.*, 2000). This maximum value is, however, significantly higher than detected by stoichiometric binding of $[^{14}\text{C}]\text{CABP}/\text{CRBP}$ in wild-type tobacco (Ruuska *et al.*, 2000). The difference is explainable by the adjustment of Rubisco content to growth conditions (for a review, see von Caemmerer and Quick, 2000). In the $-RBC$ transgenic plants, Rubisco content remained generally below 10, and typically between 2 and 5 $\mu\text{mol sites m}^{-2}$, in accordance with results reported by von Caemmerer *et al.* (1994) and Kubien and Sage (2008). Though Rubisco levels could be somewhat reduced in the $-CBF$ and $-FNR$ treatments (Palatnik *et al.*, 2003) the remaining 30–50 $\mu\text{mol sites m}^{-2}$ was well comparable with wt plants.

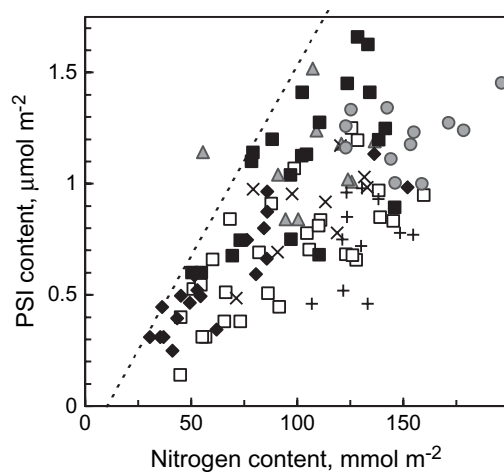


Fig. 5. Dependence of PSI content on leaf N content. The meaning of the symbols is given in Fig. 2. Dashed line indicates the maximum slope of regression.

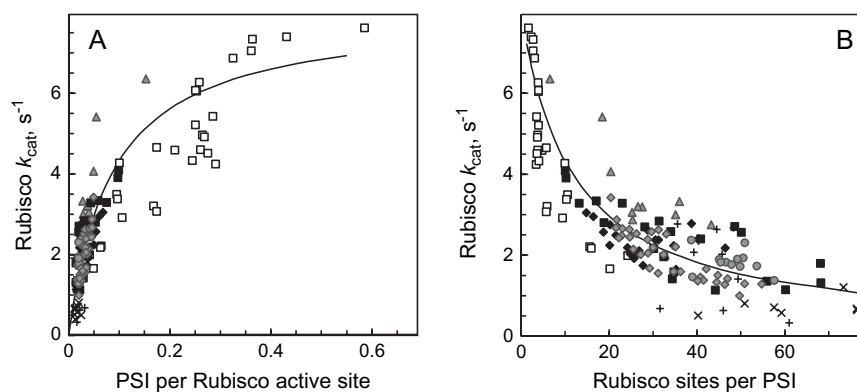


Fig. 6. Average *in planta* catalytic turnover rate, k_{cat} , of a Rubisco site as a function of PSI per Rubisco site (A) or as a function of Rubisco sites per PSI (B). The meaning of the symbols is given in Figs 2 and 3. The lines were calculated from equation (4), in (A) and equation (5) in (B).

Variation of *in planta* average k_{cat}

In wt leaves the k_{cat} values varied between 1.5 and 4 s^{-1} in tobacco (up to 6 s^{-1} in young sunflower) and increased with decreasing Rubisco content. This upper limit of k_{cat} is somewhat higher than the *in planta* value obtained for tobacco by von Caemmerer *et al.* (1994) as well as the *in vitro* values for Rubisco from tobacco (Ruuska *et al.*, 1998) and from several C_3 plants (at least those from cool habitats; Sage, 2002). The maximum value for k_{cat} of 6–7 s^{-1} observed in some leaves could be overestimated due to problems of extraction of membrane-bound Rubisco as discussed above. But this is still unlikely since the value of 6 s^{-1} has been confirmed by the data of Kubien and Sage (2008) for Rubisco in $-RBC$ tobacco. Similar high k_{cat} values (up to 8 s^{-1}) were reported in young sunflower leaves adapting from low to high growth light (Eichelmann and Laik, 1999).

The correlation between high k_{cat} values and low Rubisco content has been observed before (Quick *et al.*, 1991b; Cheng and Fuchigami, 2000) and recently documented by Kubien and Sage (2008) in -RBC tobacco, in complete agreement with our results. Similarly, the reciprocal dependence between Rubisco content and its activation state was confirmed by Suzuki *et al.* (2009), who over-expressed Rubisco in rice. But the increased Rubisco level was not accompanied by an increased photosynthetic rate, indicating lower k_{cat} in leaves where the Rubisco content was higher.

The observed variability in average k_{cat} could be (to some extent, but not all) ascribed to different carbamylation states of the enzyme. Although *in planta* and *in vitro* Rubisco activity were not compared, it is well known that the degree of carbamylation of extracted Rubisco is usually 80–90% in wt leaves under light saturating for photosynthesis at 23 °C (Butz and Sharkey, 1989; von Caemmerer *et al.*, 1994; He *et al.*, 1997; Ruuska *et al.*, 2000; Cen and Sage, 2005; Yamori *et al.*, 2006). Therefore, the wider variation of k_{cat} in our leaves (from 1.5 to 4 s⁻¹ in wt tobacco leaves and to >6 s⁻¹ in -RBC tobacco) cannot readily be explained in terms of variable carbamylation.

A novel result of this work is the relationship between Rubisco activation state and the activity of the photosynthetic electron transport chain. Expression of k_{cat} as a function of the ratio of PSI per Rubisco site revealed a hyperbolic dependence with a $K_{0.5}$ of about 0.1 PSI per Rubisco active site. In wt plants the PSI/Rubisco active site ratio varied from 0.02 to 0.1 (10 to 50 sites per PSI) with a median value of about 0.03 (33 sites per PSI). Therefore, typically the measured k_{cat} was only 20–30% of the theoretical maximum. Important new information came from the experiments with -FNR and -CBF tobacco. In control leaves grown together with the -FNR series k_{cat} was about 1.3 s⁻¹, typical for leaves with a relatively low PSI/Rubisco ratio in wt plants. In the -FNR plants Rubisco activity decreased, as was noticed by Palatnik *et al.* (2003). Quantitatively, in the -FNR plants the *in planta* apparent k_{cat} was suppressed to 0.5 s⁻¹ and correlated with the relative expression of FNR (Fig. 4A). Similarly, as soon as the expression of Cyt *b₆f* was low enough to limit electron transport, k_{cat} values decreased in strong correlation with the Cyt *b₆f*-limited electron transport rate (Fig. 4B). It is unlikely that in the -FNR case the redox control of Activase was observed, since FNR deficiency must have caused the increased reduction of ferredoxin and correspondingly more activation of Rubisco. Instead, the opposite was observed.

A shuttle model of Rubisco activase

Recent progress in understanding the mechanism of Rubisco activase has focused on interaction between Activase and Rubisco (Andrews *et al.*, 1995; Mate *et al.*, 1996; Portis, 2003; Portis *et al.*, 2008), but little new knowledge has been obtained about the interactions between Activase and thylakoid membranes since the pioneer-

ing work of Campbell and Ogren (1990, 1992). It is now known that Activase is not a simple soluble enzyme, but the protein is in reversible equilibrium between the multimer and monomer forms adsorbed on Rubisco and on thylakoid membranes. The temperature dependency of this equilibrium has been characterized (Rokka *et al.*, 2001), but little is yet known about the interactions of Activase with the components of the photosynthetic electron transport chain. Our present experiments on intact leaves do not reveal detailed molecular mechanisms, nevertheless they suggest the following kinetic model of the turnover of Rubisco activase.

The catalytic competence of Activase is lost during the activation of Rubisco, evidently because the energy-rich 'ATP form' of the protein is converted into a relatively stable 'ADP-form' as a result of the ATP-ase activity of the enzyme during the catalytic act. This inactive form of Activase requires re-activation with the help of a membrane-based nucleotide exchange factor, whose availability is in positive correlation with the components of electron transport chain, for example, ATP synthase, Cyt *b₆f*, and PSI. The activation of Activase may involve the exchange of ADP for ATP, followed by a conformational change resulting in the oligomerization. Alternatively, a (e.g. redox-activated) conformational change could be followed by binding of ATP from the solution and then oligomerization. Generally speaking, the protein is converted into the active ATP-form on the thylakoid membrane. Such conversion may, to some extent, also take place *in vitro*, in solutions and suspensions, but there the equilibrium is very sensitive to the presence of ADP, because the ADP-form of the protein is far more stable than the ATP-form.

In normal wt plants electron transport-related activation of Activase is the rate-limiting step, the step having maximum control over Rubisco activity. Less than 30% of Activase is usually activated in wt plants, as shown with the Activase-deficient transgenic tobacco, where the Activase content could be decreased by a factor of at least three before its availability became rate-limiting (Mate *et al.*, 1993, 1996). This low proportion of activated Activase is insufficient to shift the adsorption equilibrium of an unknown inhibitor to complete desorption. Usually 50–70% of Rubisco sites remain catalytically incompetent due to this inhibitor. The inhibitor seems to bind (or act) before carbamylation, leaving only a fraction of Rubisco available for further activation by carbamylation. Thus the carbamylation ratio equals the activity ratio (Butz and Sharkey, 1989), but only on the inhibitor-free sites. Since the nature of the above-discussed inhibitor is still unknown (Parry *et al.*, 1997, 2008), it may not be a chemical compound, but an inactivating conformational state of Rubisco as well, requiring chaperone-aided correction.

Independent of molecular details beyond the scope of this study, the point of this model is that the active/inactive forms of Activase are continuously shuttling between thylakoid membranes and stromally localized Rubisco, carrying the ATP-related activation factor. In our -N experiments Rubisco and PSI (and probably Activase)

decreased about proportionally and the portion of the inhibitor-free sites available for further carbamylation remained about constant when Rubisco content decreased (Fig. 3). In the -RBC transgenic plants the activity of the electron transport chain remained relatively high, although Rubisco content decreased. In these plants the turnover of Activase became Rubisco-limited and nearly all of the Rubisco was maintained in the inhibitor-free state, ensuring k_{cat} was close to its intrinsic maximum. In accordance with such a shuttle model, immunogold labelling experiments indicated that 25% of Activase was bound to thylakoids in wt rice and this fraction decreased in the anti-Activase transgenic plants where Rubisco content increased (Jin *et al.*, 2006).

Campbell and Ogren (1990, 1992) first observed that electron transport through PSI stimulated the activation of Rubisco by Activase, but it is generally believed now that, in these experiments, the underlying mechanism was based on the ATP/ADP sensitivity and redox activation of Activase (Portis, 2003). Experiments on Cyt *b₆f* deficient and GAPDH-deficient tobacco revealed that the activation of Activase was not a simple function of the ATP/ADP ratio, but the ability of Activase to detect the light signal was somehow related to Cyt *b₆f* deficiency, despite no change in the bulk ATP/ADP ratio (Ruuska *et al.*, 2000). The authors concluded that the light regulation of Rubisco by Activase is not mediated by the stromal ATP/ADP ratio or the electron transport *per se*, but, rather, by some manifestation of the balance between the photosynthetic electron transport rate and the consumption of its products, in accordance with the essence of the above shuttle model.

Physiological implications

Although the amount of Rubisco protein varies dependent on growth conditions, for example, light intensity (Walters, 2005), normally Rubisco is still disproportionately abundant in relation to the capacity of the electron transport chain. The Activase system activates such a portion of Rubisco that the RuBP carboxylation/oxygenation capacity is balanced with the electron transport capacity of the light reactions of photosynthesis. Even in plants grown at the most severe N deficiency the capacity of the electron transport chain decreases in parallel with the amount of Rubisco, always leaving a part of the Rubisco protein in inactive reserve, functioning as a storage protein (Eichelmann *et al.*, 2005). Such a strategy of N use may aim at the readiness of the plant to increase the turnover of the carbon reduction/oxidation cycle rapidly when the capacity of the electron transport system increases. The strong proportional correlation between the mesophyll conductance (initial slope of the *A* versus *C_i* curves) and maximum CO₂- and light-saturated ('potential') photosynthetic rate, observed under different environmental conditions (Eichelmann and Laisk, 1999, and references therein) and during the development of leaves (Eichelmann *et al.*, 2004b) is an old mystery, because mesophyll conductance is determined mainly by the initial slope of the Rubisco kinetic

curve (Rubisco activity), while the potential photosynthetic rate is determined by the RuBP regeneration capacity that is related to the potential of the electron transport chain. In the light of the present work we understand that Rubisco activity is under the control of the electron transport chain. Therefore, proportionality between the mesophyll conductance and the maximum CO₂ and light-saturated photosynthesis is expected. The electron transport-related control of Rubisco may shed some light also on the mysterious constancy of the *C_i/C_a* ratio (intercellular versus ambient CO₂ concentration) which stabilizes at about 0.7 under a wide variety of environmental conditions (Noormets *et al.*, 2001).

To conclude, we suggest that the empirical equation (3) approximates the data of Fig. 3 for modelling purposes. Presently, the Farquhar-von Caemmerer-Berry model (Farquhar *et al.*, 1980) is widely applied for canopy and global-scale modelling of photosynthesis. Usually Rubisco density is calculated from a correlation with N content, but k_{cat} is assumed to be constant and independent of Rubisco content. Incorporation of variable k_{cat} into the Farquhar-von Caemmerer model, dependent on leaf N (and Rubisco) content, would be a step toward a better prediction of canopy photosynthetic productivity.

Acknowledgements

This work was supported by Targeted Financing SF0180045s08 from the Estonian Ministry of Education and Science and by grants 6607 and 6611 from the Estonian Science Foundation. Co-operation with G Johnson (University of Manchester) in measurements of FNR activity and comments by R Peterson (The Connecticut Agricultural Experiment Station) concerning the manuscript are highly appreciated.

References

- Andrews TJ, Hudson GS, Mate CJ, von Caemmerer S, Evans JR, Arvidsson YBC. 1995. Rubisco: the consequences of altering its expression and activation in transgenic plants. *Journal of Experimental Botany* **46**, 1293–1300.
- Badger MR, Lorimer GH. 1976. Activation of ribulose-1,5-bisphosphate oxygenase. The role of Mg²⁺, CO₂, and pH. *Archives of Biochemistry and Biophysics* **175**, 723–729.
- Boyle FA, Keys AJ. 1987. The state of activation of ribulose-1, 5-bisphosphate carboxylase in wheat leaves. *Photosynthesis Research* **11**, 97–108.
- Burnette WN. 1981. 'Western blotting': electrophoretic transfer of proteins from sodium dodecyl sulfate-polyacrylamide gels to unmodified nitrocellulose and radiographic detection with antibody and radioiodinated protein A. *Analytical Biochemistry* **112**, 195–203.
- Butz ND, Sharkey TD. 1989. Activity ratios of ribulose-1, 5-bisphosphate carboxylase accurately reflect carbamylation ratios. *Plant Physiology* **89**, 735–739.

- Campbell WJ, Ogren WL.** 1990. Electron transport through photosystem I stimulates light activation of ribulose biphosphate carboxylase/oxygenase (Rubisco) by Rubisco activase. *Plant Physiology* **94**, 479–484.
- Campbell WJ, Ogren WL.** 1992. Light activation of Rubisco by Rubisco activase and thylakoid membranes. *Plant and Cell Physiology* **33**, 751–756.
- Gen Y-P, Sage RF.** 2005. The regulation of Rubisco activity in response to variation in temperature and atmospheric CO₂ partial pressure in sweet potato. *Plant Physiology* **139**, 979–990.
- Cheng L, Fuchigami LH.** 2000. Rubisco activation state decreases with increasing nitrogen content in apple leaves. *Journal of Experimental Botany* **51**, 1687–1694.
- Edmondson DL, Badger MR, Andrews TJ.** 1990a. A kinetic characterization of slow inactivation of ribulose biphosphate carboxylase during catalysis. *Plant Physiology* **93**, 1376–1382.
- Edmondson DL, Badger MR, Andrews TJ.** 1990b. Slow inactivation of ribulose biphosphate carboxylase during catalysis is not due to decarbamylation of the catalytic site. *Plant Physiology* **93**, 1383–1389.
- Eichelmann H, Laisk A.** 1990. Ribulose-1,5-bisphosphate carboxylase content and kinetic characteristics of photosynthesis in leaves. *Fiziologija Rastenii (Soviet Plant Physiology)* **37**, 1053–1064.
- Eichelmann H, Laisk A.** 1999. Ribulose-1,5-bisphosphate carboxylase/oxygenase content, assimilatory charge and mesophyll conductance in leaves. *Plant Physiology* **119**, 179–189.
- Eichelmann H, Oja V, Rasulov B, Padu E, Bichele I, Pettai H, Mänd P, Kull O, Laisk A.** 2005. Adjustment of leaf photosynthesis to shade in a natural canopy: reallocation of nitrogen. *Plant, Cell and Environment* **28**, 389–401.
- Eichelmann H, Oja V, Rasulov B, Padu E, Bichele I, Pettai H, Möls T, Kasparova I, Vapaavuori E, Laisk A.** 2004a. Photosynthetic parameters of birch (*Betula pendula* Roth) leaves growing in normal and in CO₂- and O₃- enriched atmospheres. *Plant, Cell and Environment* **27**, 479–495.
- Eichelmann H, Oja V, Rasulov B, Padu E, Bichele I, Pettai H, Niinemets Ü, Laisk A.** 2004b. Development of leaf photosynthetic parameters in *Betula pendula* Roth leaves: correlations with photosystem I density. *Plant Biology* **6**, 307–318.
- Farquhar GD, von Caemmerer S, Berry JA.** 1980. A biochemical model of photosynthetic CO₂ assimilation in leaves of C₃ species. *Planta* **149**, 78–90.
- Graan T, Ort DR.** 1984. Quantitation of the rapid electron donors to P700, the functional plastoquinone pool, and the ratio of the photosystems in spinach chloroplasts. *Journal of Biological Chemistry* **259**, 14003–14010.
- Hajirezaei M-R, Peisker M, Tschiersch H, Palatnik JF, Valle EM, Carillo N, Sonnewald U.** 2002. Small changes in the activity of chloroplastic NADP⁺-dependent ferredoxin oxidoreductase lead to impaired plant growth and restrict photosynthetic activity of transgenic tobacco plants. *The Plant Journal* **29**, 281–293.
- Harley PC, Loreto F, Di Marco G, Sharkey TD.** 1992. Theoretical considerations when estimating the mesophyll conductance to CO₂ flux by analysis of the response of photosynthesis to CO₂. *Plant Physiology* **98**, 1429–1436.
- He Z, von Caemmerer S, Hudson GS, Price GD, Badger MR, Andrews TJ.** 1997. Ribulose-1,5-bisphosphate carboxylase/oxygenase activase deficiency delays senescence of ribulose-1,5-bisphosphate carboxylase/oxygenase but progressively impairs its catalysis during tobacco leaf development. *Plant Physiology* **115**, 1569–1580.
- Hiyama T.** 1985. Quantum yield and requirement for the photooxidation of P700. *Physiologia Vegetale* **23**, 605–610.
- Hiyama T, Ke B.** 1972. Difference spectra and extinction coefficients of P₇₀₀. *Biochimica et Biophysica Acta* **267**, 160–171.
- Hudson GS, Evans JR, von Caemmerer S, Arvidsson YBC, Andrews TJ.** 1992. Reduction of ribulose-1,5-bisphosphate carboxylase/oxygenase content by antisense RNA reduces photosynthesis in transgenic tobacco plants. *Plant Physiology* **98**, 294–302.
- Jin S-H, Hong J, Li X-Q, Jiang D-A.** 2006. Antisense inhibition of Rubisco activase increases Rubisco content and alters the proportion of Rubisco activase in stroma and thylakoids in chloroplasts of rice leaves. *Annals of Botany* **97**, 739–744.
- Jordan DB, Chollet R, Ogren WL.** 1983. Binding of phosphorylated effectors by active and inactive forms of ribulose-1,5-bisphosphate carboxylase. *Biochemistry* **22**, 3410–3418.
- Knight S, Andersson I, Branden CI.** 1990. Crystallographic analysis of ribulose 1,5-bisphosphate carboxylase from spinach at 2.4 Å resolution. Subunit interactions and active site. *Journal of Molecular Biology* **215**, 113–160.
- Kubien DS, Sage RF.** 2008. The temperature response of photosynthesis in tobacco with reduced amounts of Rubisco. *Plant, Cell and Environment* **31**, 407–418.
- Laisk A, Eichelmann H, Oja V, Rasulov B, Padu E, Bichele I, Pettai H, Kull O.** 2005. Adjustment of leaf photosynthesis to shade in natural canopy: rate parameters. *Plant, Cell and Environment* **28**, 375–388.
- Laisk A, Eichelmann H, Oja V, Talts E, Scheibe R.** 2007. Rates and roles of cyclic and alternative electron flow in potato leaves. *Plant and Cell Physiology* **48**, 1575–1588.
- Laisk A, Oja V.** 1974. Leaf photosynthesis in short pulses of CO₂. The carboxylation reaction *in vivo*. *Fiziologija Rastenii (Soviet Plant Physiology)* **21**, 1123–1131 (in Russian).
- Laisk A, Oja V.** 1998. *Dynamic gas exchange of leaf photosynthesis. Measurement and interpretation*. Collingwood: CSIRO Publishing.
- Laisk A, Oja V, Rasulov B, Rämme H, Eichelmann H, Kasparova I, Pettai H, Padu E, Vapaavuori E.** 2002. A computer-operated routine of gas exchange and optical measurements to diagnose photosynthetic apparatus in leaves. *Plant, Cell and Environment* **25**, 923–943.
- Lilley RM, Portis AR.** 1997. ATP hydrolysis activity and polymerization state of ribulose-1,5-bisphosphate carboxylase oxygenase activase. *Plant Physiology* **114**, 605–613.
- Makino A, Nakano H, Mae T, Shimada T, Yamamoto N.** 2000. Photosynthesis, plant growth and N allocation in transgenic rice plants with decreased Rubisco under CO₂ enrichment. *Journal of Experimental Botany* **51**, 383–389.
- Makino A, Osmond B.** 1991. Solubilization of ribulose-1,5-bisphosphate carboxylase from the membrane fraction of pea leaves. *Photosynthesis Research* **29**, 79–85.

- Mate CJ, Hudson GS, von Caemmerer S, Evans JR, Andrews TJ.** 1993. Reduction of ribulose biphosphate carboxylase activase levels in tobacco (*Nicotiana tabacum*) by antisense RNA reduces ribulose biphosphate carboxylase carbamylation and impairs photosynthesis. *Plant Physiology* **102**, 1119–1128.
- Mate CJ, von Caemmerer S, Evans JR, Hudson GS, Andrews TJ.** 1996. The relationship between CO₂-assimilation rate, Rubisco carboxylation and Rubisco activase content in activase-deficient transgenic tobacco suggest a simple model of activase action. *Planta* **198**, 604–613.
- Noormets A, Söber A, Pell EJ, Dickson RE, Podila GK, Söber J, Isebrands JG, Karnosky DF.** 2001. Stomatal and non-stomatal limitation to photosynthesis in two trembling aspen (*Populus tremuloides* Michx.) clones. *Plant, Cell and Environment* **24**, 327–336.
- Oja V, Eichelmann H, Peterson RB, Rasulov B, Laisk A.** 2003. Decyphering the 820 nm signal: redox state of donor side and quantum yield of photosystem I in leaves. *Photosynthesis Research* **78**, 1–15.
- Oja V, Bichele I, Hüve K, Rasulov B, Laisk A.** 2004. Reductive titration of photosystem I and differential extinction coefficient of P700⁺ at 810–950 nm in leaves. *Biochimica et Biophysica Acta* **1658**, 225–234.
- Palatnik JF, Tognetti VB, Poli HO, Rodriguez RE, Blanco N, Gattuso M, Hajirezaei M-R, Sonnewald U, Valle EM, Carrillo N.** 2003. Transgenic tobacco plants expressing antisense ferredoxin-NADP(H) reductase transcripts display increased susceptibility to photo-oxidative damage. *The Plant Journal* **35**, 332–341.
- Parry MA, Andralojc PJ, Parmar S, Keys AJ, Habash D, Paul MJ, Alred R, Quick WP, Servaites JC.** 1997. Regulation of Rubisco by inhibitors in the light. *Plant, Cell and Environment* **20**, 528–534.
- Parry MA, Andralojc PJ, Mitchell RAC, Madgwick PJ, Keys AJ.** 2003. Manipulation of Rubisco: the amount, activity, function, and regulation. *Journal of Experimental Botany* **54**, 1321–1333.
- Parry MAJ, Keys AJ, Madgwick PJ, Carmo-Silva AE, Andralojc PJ.** 2008. Rubisco regulation: a role for inhibitors. *Journal of Experimental Botany* **59**, 1569–1580.
- Portis Jr AR.** 1992. Regulation of ribulose 1,5-bisphosphate carboxylase/oxygenase activity. *Annual Review of Plant Physiology and Plant Molecular Biology* **43**, 415–437.
- Portis AR.** 2003. Rubisco activase: Rubisco's catalytic chaperone. *Photosynthesis Research* **75**, 11–27.
- Portis ARJ, Li S, Wang D, Salvucci ME.** 2008. Regulation of Rubisco activase and its interaction with Rubisco. *Journal of Experimental Botany* **59**, 1957–1604.
- Price GD, Yu JW, von Caemmerer S, Evans JR, Chow WS, Anderson JM, Hurry V, Badger MR.** 1995. Chloroplast cytochrome *b₆/f* and ATP synthase complexes in tobacco: transformation with antisense RNA against nuclearencoded transcripts for the Rieske FeS and ATPs polypeptides. *Australian Journal of Plant Physiology* **22**, 285–297.
- Quick WP, Schurr U, Fichtner K, Schulze E-D, Rodermeel SR, Bogorad L, Stitt M.** 1991a. The impact of decreased Rubisco on photosynthesis, growth, allocation and storage in tobacco plants which have been transformed with antisense *rbcS*. *The Plant Journal* **1**, 51–58.
- Quick WP, Schurr U, Scheibe R, Schulze E-D, Rodermeel SR, Bogorad L, Stitt M.** 1991b. Decreased ribulose-1,5-bisphosphate carboxylase-oxygenase in transgenic tobacco transformed with 'antisense' *rbcS*. II. Flux control coefficients for photosynthesis in varying light, CO₂, and air humidity. *Planta* **183**, 555–566.
- Robinson SP, Portis AR.** 1989. Ribulose-1,5-bisphosphate carboxylase/oxygenase activase protein prevents the *in vitro* decline in activity of ribulose-1,5-bisphosphate carboxylase/oxygenase. *Plant Physiology* **90**, 968–971.
- Rokka A, Zhang L, Aro E-M.** 2001. Rubisco activase: an enzyme with a temperature-dependent dual function. *The Plant Journal* **25**, 463–471.
- Ruuska S, Andrews JT, Badger MR, Hudson GS, Laisk A, Price D, von Caemmerer S.** 1998. The interplay between limiting processes in C₃ photoynthesis studied by rapid-response gas exchange using transgenic tobacco impaired in photosynthesis. *Australian Journal of Plant Physiology* **25**, 859–870.
- Ruuska SA, Andrews TJ, Badger MR, Price GD, von Caemmerer S.** 2000. The role of chloroplast electron transport and metabolites in modulating Rubisco activity in tobacco. Insights from transgenic plants with reduced amounts of cytochrome *b/f* complex or glyceraldehyde 3-phosphate dehydrogenase. *Plant Physiology* **122**, 491–504.
- Sage RF.** 2002. Variation in the *k_{cat}* of Rubisco in C₃ and C₄ plants and some implications for photosynthetic performance at high and low temperature. *Journal of Experimental Botany* **53**, 609–620.
- Sage RF, Seemann JR.** 1993. Regulation of ribulose-1,5-bisphosphate carboxylase/oxygenase activity in response to reduced light intensity in C₄ plants. *Plant Physiology* **102**, 21–28.
- Salvucci ME, Werneke JM, Ogren WL, Portis Jr AR.** 1987. Purification and species distribution of Rubisco activase. *Plant Physiology* **84**, 930–936.
- Sharkey T.** 2005. Effects of moderate heat stress on photosynthesis: importance of thylakoid reactions, rubisco deactivation, reactive oxygen species, and thermotolerance provided by isoprene. *Plant, Cell and Environment* **28**, 269–277.
- Sharkey TD, Badger MR, von Caemmerer S, Andrews TJ.** 2001. Increased heat sensitivity of photosynthesis in tobacco with reduced Rubisco activase. *Photosynthesis Research* **67**, 147–156.
- Suzuki Y, Miyamoto T, Yoshizawa R, Mae T, Makino A.** 2009. Rubisco content and photosynthesis of leaves at different positions in transgenic rice with an overexpression of *RBCS*. *Plant, Cell and Environment* **32**, 417–427.
- Tcherkez GGB, Farquhar GD, Andrews TJ.** 2006. Despite slow catalysis and confused substrate specificity, all ribulose biphosphate carboxylases may be nearly perfectly optimized. *Proceedings of the National Academy of Sciences, USA* **103**, 7246–7251.
- von Caemmerer S, Evans JR, Hudson GS, Andrews TJ.** 1994. The kinetics of ribulose-1,5-bisphosphate carboxylase/oxygenase *in vivo* inferred from measurements of photosynthesis in leaves of transgenic tobacco. *Planta* **195**, 88–97.
- von Caemmerer S, Quick WP.** 2000. Rubisco: physiology *in vivo*. In: Leegood RC, Sharkey TD, von Caemmerer S, eds. *Photosynthesis: physiology and metabolism*. The Netherlands: Kluwer Academic Publishers, 85–113.

Vu JCV, Allen LH, Bowes G. 1984. Dark/light modulation of ribulose-1,5-bisphosphate carboxylase activity in plants from different photosynthetic categories. *Plant Physiology* **76**, 843–845.

Walters RG. 2005. Towards an understanding of photosynthetic acclimation. *Journal of Experimental Botany* **56**, 435–447.

Yamori W, Suzuki K, Noguchi K, Nakai M, Terashima I. 2006. Effects of Rubisco kinetics and Rubisco activation state on the temperature dependence of the photosynthetic rate in spinach leaves from contrasting growth temperatures. *Plant, Cell and Environment* **29**, 1659–1670.

Yokota A, Kitaoka S. 1985. Correct pK values for dissociation constant of carbonic acid lower the reported K_m values of ribulose

bisphosphate carboxylase by half. Presentation of a nomograph and an equation for determining the pK values. *Biochemical and Biophysical Research Communications* **131**, 1075–1079.

Zhang N, Kallis RP, Ewy RG, Portis Jr AR. 2002. Light modulation of Rubisco in *Arabidopsis* requires a capacity for redox regulation of the larger Rubisco activase isoform. *Proceedings of the National Academy of Sciences, USA* **99**, 3330–3334.

Zhang N, Portis AR. 1999. Mechanism of light regulation of Rubisco: a specific role for the larger Rubisco activase isoform involving reductive activation by thioredoxin-f. *Proceedings of the National Academy of Sciences, USA* **96**, 9438–9443.